Correlations between Ca II H&K Emission and the Gaia M dwarf Gap

Emily M. Boudreaux,[1] Aylin Garcia Soto,[1] and Brian C. Chaboyer[1]

[1]*Department of Physics and Astronomy, Dartmouth College, Hanover, NH 03755, USA*

ABSTRACT

The Gaia M dwarf gap, also known as the Jao Gap, is a novel feature discovered in the Gaia DR2 G vs. BP-RP color magnitude diagram. This gap represents a 17 percent decrease in stellar density in a thin magnitude band around the convective transition mass ($\sim 0.35 M_\odot$) on the main sequence. Previous work has demonstrated a paucity of Hydrogen Alpha emission coincident with the G magnitude of the Jao Gap in the solar neighborhood. The exact mechanism which results in this paucity is as of yet unknown; however, the authors of the originating paper suggest that it may be the result of complex variations to a star's magnetic topology driven by the Jao Gap's characteristic formation and breakdown of stars' radiative transition zones. We present a follow up investigating another widely used magnetic activity metric, Calcium II H&K emission. Ca II H&K activity appears to share a similar anomalous behavior as Hα does near the Jao Gap magnitude. We observe an increase in star-to-star variation of magnetic activity near the Jao Gap. **We present a toy model of a stars magnetic field evolution which demonstrates that** this increase may be due to stochastic disruptions to the magnetic field originating from the periodic mixing events characteristic of the convective kissing instabilities which drive the formation of the Jao Gap.

1. INTRODUCTION

The initial mass requirements of molecular clouds collapsing to form stars results in a strong bias towards lower masses and later spectral classes during star formation. Partly as a result of this bias and partly as a result of their extremely long main-sequence lifetimes, M Dwarfs make up approximately 70 percent of all stars in the galaxy (Winters et al. 2019). Moreover, many planet search campaigns have focused on M Dwarfs due to the relative ease of detecting small planets in their habitable zones (e.g. Nutzman & Charbonneau 2008). M Dwarfs then represent both a key component of the galactic stellar population as well as the most numerous possible set of stars which may host habitable exoplanets. Given this key location M Dwarfs occupy in modern astronomy it

Corresponding author: Emily M. Boudreaux
emily.m.boudreaux.gr@dartmouth.edu,
emily@boudreauxmail.com

is important to have a thorough understanding of their structure and evolution.

Jao et al. (2018) discovered a novel feature in the Gaia Data Release 2 (DR2) $G_{BP} - G_{RP}$ color-magnitude-diagram. Around $M_G = 10$ there is an approximately 17 percent decrease in stellar density of the sample of stars Jao et al. (2018) considered. Subsequently, this has become known as either the Jao Gap, or Gaia M Dwarf Gap. Following the initial detection of the Gap in DR2 the Gap has also potentially been observed in 2MASS (Skrutskie et al. 2006; Jao et al. 2018); however, the significance of this detection is quite weak and it relies on the prior of the Gap's location from Gaia data. The Gap is also present in Gaia Early Data Release 3 (EDR3) (Jao & Feiden 2021). These EDR3 and 2MASS data sets then indicate that this feature is not a bias inherent to DR2.

The Gap is generally attributed to convective instabilities in the cores of stars straddling the fully convective transition mass (0.3 - 0.35 M$_\odot$) **known as convective kissing instabilities** (Baraffe & Chabrier 2018). These

instabilities interrupt the normal, slow, main sequence luminosity evolution of a star and result in luminosities lower than expected from the main sequence mass-luminosity relation (Jao & Feiden 2020).

The Jao Gap, inherently a feature of M Dwarf populations, provides an enticing and unique view into the interior physics of these stars (Feiden et al. 2021). This is especially important as, unlike more massive stars, M Dwarf seismology is infeasible due to the short periods and extremely small magnitudes which both radial and low-order low-degree non-radial seismic waves are predicted to have in such low mass stars (Rodríguez-López 2019). The Jao Gap therefore provides one of the only current methods to probe the interior physics of M Dwarfs.

The magnetic activity of M dwarfs is of particular interest due to the theorised links between habitability and the magnetic environment which a planet resides within (e.g. Lammer et al. 2012; Gallet et al. 2017; Kislyakova et al. 2017). M dwarfs are known to be more magnetically active than earlier type stars (Saar & Linsky 1985; Astudillo-Defru et al. 2017; Wright et al. 2018) while simultaneously this same high activity calls into question the canonical magnetic dynamo believed to drive the magnetic field of solar-like stars (the $\alpha\Omega$ dynamo) (Shulyak et al. 2015). One primary challenge which M dwarfs pose is that stars less than approximately 0.35 $M_\odot$ are composed of a single convective region. This denies any dynamo model differential rotation between adjacent levels within the star. Alternative dynamo models have been proposed, such as the α^2 dynamo along with modifications to the $\alpha\Omega$ dynamo which may be predictive of M dwarf magnetic fields (Chabrier & Küker 2006; Kochukhov 2021; Kleeorin et al. 2023).

Despite this work, very few studies have dived specifically into the magnetic field of M dwarfs at or near the convective transition region . This is not surprising as that only spans approximately a 0.2 magnitude region in the Gaia BP-RP color magnitude diagram and is therefore populated by a relatively small sample of stars.

Jao et al. (2023) identify the Jao Gap as a strong discontinuity point for magnetic activity in M dwarfs. Two primary observations from their work are that the Gap serves as a boundary where very few active stars, in their sample of 640 M dwarfs, exist below the Gap and that the overall downward trend of activity moving to fainter magnitudes is anomalously high in within the 0.2 mag range of the Gap. Jao et al. Figures 3 and 13 make this paucity in Hα emission particularly clear. Based on previous work from Spada & Lanzafame (2020); Curtis et al. (2020); Dungee et al. (2022) the authors propose that the mechanism resulting in the reduced fraction of active stars within the Gap is that as the radiative zone dissipates due to core expansion, angular momentum from the outer convective zone is dumped into the core resulting in a faster spin down than would otherwise be possible. Effectively the core of the star acts as a sink, reducing the amount of angular momentum which needs to be lost by magnetic breaking for the outer convective region to reach the same angular velocity. Given that Hα emission is strongly coupled magnetic activity in the upper chromosphere (Newton et al. 2016; Kumar et al. 2023) and that a star's angular velocity is a primary factor in its magnetic activity, a faster spin down will serve to more quickly dampen Hα activity.
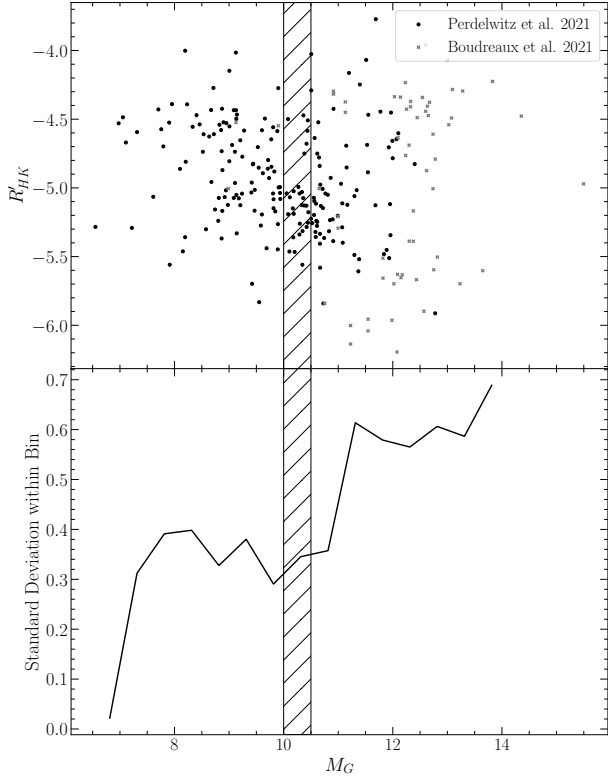
In addition to Hα the Calcium Fraunhaufer lines may be used to trace the magnetic activity of a star. These lines originate from magnetic heating of the lower chromosphere driven by magnetic shear stresses within the star. Both Perdelwitz et al. (2021) and Boudreaux et al. (2022) present calcium emission measurements for stars spanning the Jao Gap. In this paper we search for similar trends in the Ca II H& K emission as Jao et al. see in the Hα emission. In Section 2 we investigate the empirical star-to-star variability in emission and quantify if this could be due to noise or sample bias; in Section 3 we present a simplified toy model which shows that the mixing events characteristic of convective kissing instabilities could lead to increased star-to-star variability in activity as is seen empirically.
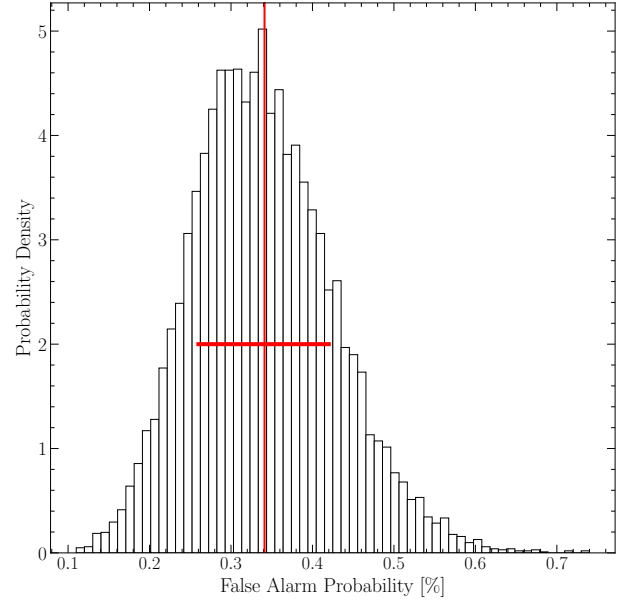
2. CORRELATION

Using Ca II H&K emission data from Perdelwitz et al. (2021) and Boudreaux et al. (2022) (quantified using the R'_{HK} metric Middelkoop 1982; Rutten 1984) we investigate the correlation between the Jao Gap magnitude and stellar magnetic activity. We are more statistically limited here than past authors have been due to the requirement for high resolution spectroscopic data when measuring Calcium emission.

The merged dataset is presented in Figure 1. **The sample overlap between Perdelwitz et al. (2021) and Boudreaux et al. (2022) is small (only consisting of five targets). For those five targets there is an approximately 1.5 percent average difference between measured $\log(R'_{HK})$ values, with measurements from Boudreaux et al. biased to be slightly more negative than those from Perdelwitz et al.**

There is a visual discontinuity in **the spread of stellar activity** below the Jao Gap magnitude. **Further discussion of why there may be disagreement between the observed magnitude of the gap and the discontinuity which we identify may be found in**

Figure 1. Merged Dataset from Perdelwitz et al. (2021); Boudreaux et al. (2022). Note the increase in the spread of R'_{HK} around the Jao Gap Magnitude **(top). Standard deviation of Calcium emission data within each bin. Note the discontinuity near the Jao Gap Magnitude (bottom). The location of the Gap as identified in literature is shown by the hatched region ($\sim$ 10-10.5 M_G). Potential explanations for the disagreement in magnitude are discussed in detail in Section 2.1.**
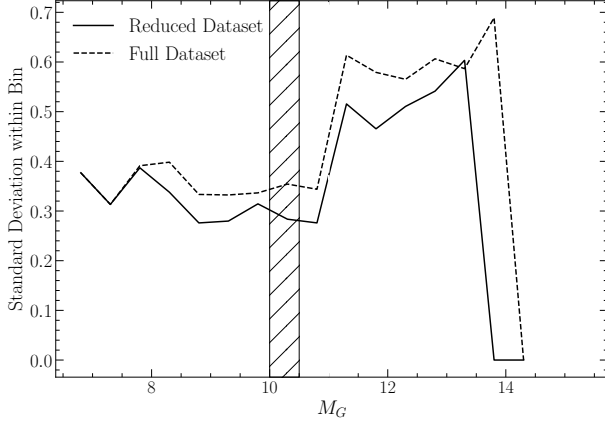
Section 2.1. In order to quantify the significance of this discontinuity we measure the false alarm probability of the change in standard deviation.

First we split the merged dataset into bins with a width of 0.5 mag. In each bin we measure the standard deviation about the mean of the data. The results of this are shown in Figure 1 (bottom). In order to measure the false alarm probability of this discontinuity we first resample the merged calcium emission data based on the associated uncertainties for each datum as presented in their respective publications. Then, for each of these "resample trials" we measure the probability that a change in the standard deviation of the size seen would happen purely due to noise. Results of this test are show in in Figure 2.
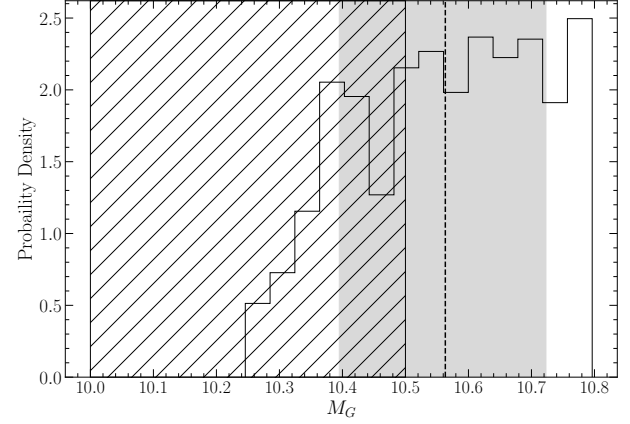
This rapid increase star-to-star variability would only arise due purely to noise 0.3 ± 0.08 percent of the time and is therefore likely either a true effect or an alias of some sample bias.

Figure 2. Probability distribution of the false alarm probability for the discontinuity seen in Figure 1. The mean of this distribution is $0.341\%\pm^{0.08}_{0.08}$.

If the observed increase in variability is not due to a sample bias and rather is a physically driven effect then there is an obvious similarity between these findings and those of Jao et al. (2023). Specifically we find a increase in variability below the magnitude of the Gap. Moreover, this variability increase is primarily driven by an increase in the number of low activity stars (as opposed to an increase in the number of high activity stars). We can further investigate the observed change in variability for only low activity stars by filtering out those stars at or above the saturated threshold for magnetic activity. Boudreaux et al. (2022) identify $\log(R'_{HK}) = -4.436$ as the saturation threshold. We adopt this value and filter out all stars where $\log(R'_{HK}) \geq -4.436$. Applying the same analysis to this reduced dataset as was done to the full dataset we still find a discontinuity at the same location (Figure 3). This discontinuity is of a smaller magnitude and consequently is more likely to be due purely to noise, with a 7 ± 0.2 percent false alarm probability. This false alarm probability is however only concerned with the first point after the jump in variability. If we consider the false alarm probability of the entire high variability region then the probability that the high variability region is due purely to noise drops to 1.4 ± 0.04 percent.

Further, various authors have shown that the strength of Calcium II H&K emission may evolve over month to year timescales (e.g. Rauscher & Marcy 2006; Perdelwitz et al. 2021; Cretignier et al. 2024). Targets from Boudreaux et al.

Figure 3. Spread in the magnetic activity metric for the merged sample with any stars $\log(R'_{HK}) > -4.436$ filtered out. **The location of the Gap as identified in literature is shown by the hatched region ($\sim$ 10-10.5 M_G).**

Figure 4. Probability density distribution of discontinuity location as identified in the merged dataset. The dashed line represents the mean of the distribution while the shaded region runs from the 16th percentile to the 84th percentile of the distribution. This distribution was built from 10,000 independent samples where the discontinuity was identified as the highest value in the gradient of the standard deviation. **The location of the Gap as identified in literature is shown by the hatched region ($\sim$ 10-10.5 M_G).**

(2022) were observed an average of only four times and over year long timescales. Therefore, the nominal $\log(R'_{HK})$ values derived in that work may be biased by stellar variability. However, the scale of observed variabilty in the activity metric is signifigantly smaller than the star-to-star activity variability addressed here and therfore activity cycles are not expected to be of particular relevance. Specifically, the amplitude of variability is generally $\Delta \log(R'_{HK}) \lessapprox 0.2$ wherase in this work we address variability on the order of $\Delta \log(R'_{HK}) \lessapprox 2$.

We observe a strong, likely statistically significant, discontinuity in the star-to-star variability of Ca II H&K emission below the magnitude of the Jao Gap. However, modeling is required to determine if this discontinuity may be due to the same underlying physics.

2.1. Conicidence with the Jao Gap Magnitude

While the observed increase in variability seen here does not seem to be coincident with the Jao Gap — instead appearing to be approximately 0.5 mag fainter, in agreement with what is observed in Jao et al. (2023) — a number of complicating factors prevent us from falsifying that the these two features are not coincident. Jao et al. find, similar to the results presented here, that the paucity of $H\alpha$ emission originates below the Gap. Moreover, we use a 0.5 magnitude bin size when measuring the star-to-star variability which injects error into the positioning of any feature in magnitude space. We can quantify the degree of uncertainty the magnitude bin choice injects by conducting Monte Carlo trials where bins are randomly shifted redder or bluer. We conduct 10,000 trials where each trial involves sampling

a random shift to the bin start location from a normal distribution with a standard deviation of 1 magnitude. For each trial we identify the discontinuity location as the maximum value of the gradient of the standard deviation (this is the derivative of the data in Figures **??** & 3). Some trials result in the maximal value lying at the 0th index of the magnitude array due to edge effects, these trials are rejected (and account for 11% of the trials). The uncertainty in the identified magnitude of the discontinuity due to the selected start point of the magnitude bins reveals a $1\sigma = \pm0.32$ magnitude uncertainty in the location of the discontinuity (Figure 4). Finally, all previous studies of the M dwarf Gap (Jao et al. 2018; Jao & Feiden 2021; Mansfield & Kroupa 2021; Boudreaux et al. 2022; Jao et al. 2023) demonstrate that the Gap has a color dependency, shifting to fainter magnitudes as the population reddens and consequently an exact magnitude range is ill-defined. Therefore we cannot falsify the model that the discontinuity in star-to-star activity variability is coincident with the Jao Gap magnitude.

2.2. Rotation

It is well known that star's magnetic activity tend to be correlated with their rotational velocity (Vaughan et al. 1981; Newton et al. 2016; Astudillo-Defru et al. 2017; Houdebine et al. 2017; Boudreaux et al. 2022); therefore, we investigate whether there is a similar correlation between Gap location and rotational period in our dataset. All targets from Boudreaux et al. (2022)

already have published rotational periods; however, targets from Perdelwitz et al. (2021) do not necessarily have published periods. Therefore, we derive photometric rotational periods for these targets here. Given the inherent heterogeneity of M Dwarf stellar surfaces (Boisse et al. 2011; Robertson et al. 2020) we are able to determine the rotational period of a star through the analysis of active regions. Various methodologies can be employed for this purpose, including the examination of photometry and light curves (e.g., Newton et al. 2016), and the observation of temporal changes in the strength of chromospheric emission lines such as Ca II H & K or Hα (e.g., Fuhrmeister et al. 2019; Kumar & Fares 2023). In this work, new rotational periods are derived from TESS 2-minute cadence data[1].

Due to both the large frequency and amplitudes of M dwarf flaring rates the photometric period can prove difficult to measure — as frequency directly correlates with periodicity. Thus, following the process described in García Soto et al. (2023), we utilize two methods in this paper to reduce the effect of flares. One method uses `stella` a python package which implements a series of pre-trained convolutional neural networks (CNNs) to remove flare-shaped features in a light curve (Feinstein et al. 2020a). The second method separates a star's photometry into 10 minute bins to account for misshapen flares which `stella` is known to be biased against detecting.

`stella` employs a diverse library of models trained with varying initial seeds (Feinstein et al. 2020b,a). The Convolutional Neural Networks in `stella` are trained on labeled TESS 2-min for both flares and non-flares. For the purposes of this paper, we use an ensemble of 100 models in `stella`'s library to optimize model performance (Feinstein et al. 2020b, for further detail). `stella` scores flairs with a probability of between 0 to 1 — where higher values indicate a higher confidence that a feature is a flare. Here we adopt a score of 0.5 as the cutoff threshold, all features with a score of 0.5 or greater are classed as flares and removed (e.g. Feinstein et al. 2020b).

Furthermore, we also bin the data from a 2-min to 10-min cadence using the python package `lightkurve`'s binning function (Lightkurve Collaboration et al. 2018; Barentsen et al. 2020). This further reduces any flaring-contribution that might have been missed by `stella`[2]. Subsequently, we filter photometry, only retaining data whos residuals are less than 4 times the root-mean-square deviation.

Gaussian processes for modeling the periods are based on Angus et al. (2018) for the subset of M Dwarfs with no fiducial periods. The `starspot` package is adapted for light curve analysis (Angus 2021; Angus & Garcia Soto 2023). Our Gaussian process kernel function incorporates two stochastically-driven simple harmonic oscillators, representing primary ($P_{\rm rot}$) and secondary ($P_{\rm rot}/2$) rotation modes. First, we implement the Lomb-Scargle periodogram within `starspot` to initially estimate the period. After which, we create a maximum a posteriori (MAP) fit using `starspot` to generate a model for stellar rotation. To obtain the posterior of the stellar rotation model, we use Markov Chain Monte Carlo (MCMC) sampling using the `pymc3` package (Salvatier et al. 2016) within our adapted `starspot` version. All rotational periods are presented in Table 1. Our final sample contains 187 stars with measured rotational periods. We derive new rotational periods for 7 of these.

One might expect a decrease in mean rotational period around the magnitude of the Gap, due to the slight decrease in magnetic activity. However, there is no statistically significant correlation between rotational period and G magnitude which we can detect given our sample size (Figure 5). Rotational period is however, not the ideal parametrization to use, as magnetic activity is more directly related to the Rossby number (Ro). Using the empirical calibration presented in Wright et al. (2018) (Equation 1) we find the mixing timescale for each star such that the Rossby Number is defined as $Ro = P_{rot}/\tau_c$.

$$\tau_c = 0.64 + 0.25 * (V - K) \qquad (1)$$

When we compare Rossby number to G magnitude (Figure 6) we find that there may be a slight paucity of rotation coincident with the decrease in spread of the activity metric. We quantify the statistical significance of this drop by building a Gaussian kernel density estimator (kde) based on the data outside of this range, and then resampling that kde 10000 times for each data point in the theorized paucity range. The false alarm probability that that drop is due to noise is then the product of the fraction of samples which are less than or equal to the value of each data point. We find that there is a 0.022 percent probability that this dip is due purely to noise.
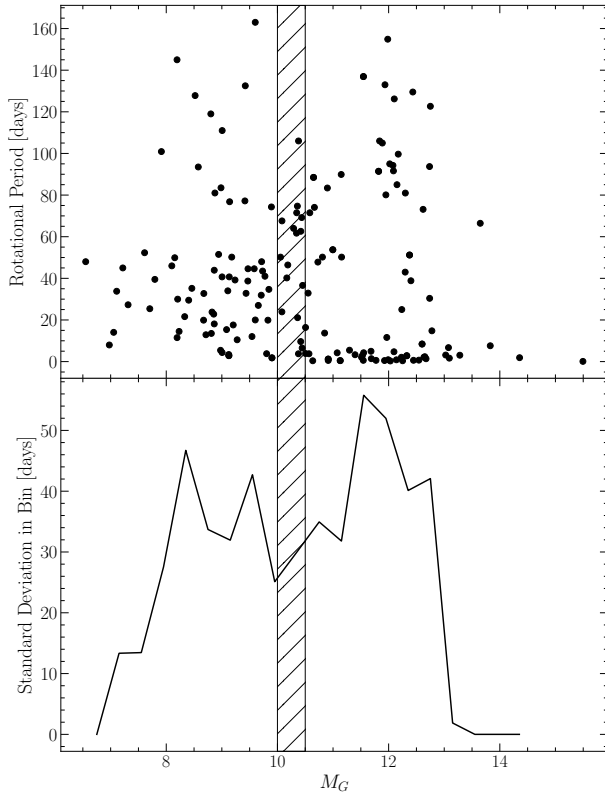
2.3. *Limitations*

There are two primary limitation of our dataset. First, we only have 264 star in our dataset (with measured R'_{HK}, 187 with rotational periods) limiting the statis-

---

[1] Some M Dwarfs lacking a documented rotational period did not have sufficient TESS data to yield fiducial rotational periods
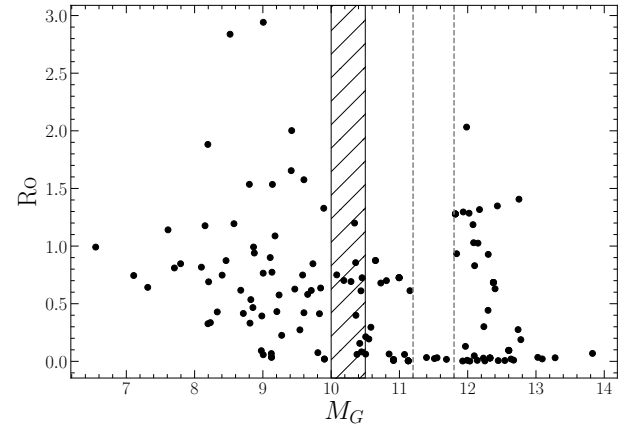
[2] This is relevant for flares that are misshapen at the start or break in the dataset due to missing either the ingress or egress.

ID	G Mag	V Mag	K Mag	$\log(R'_{HK})$	e_Log(R'$_{HK}$)	Ro	prot	r_prot
	mag	mag	mag				d	
2MASS J00094508-4201396	12.14	13.659	8.223	-4.339	0.001	0.009	0.859	Bou22
2MASS J00310412-7201061	12.301	13.648	8.445	-5.388	0.003	0.928	80.969	Bou22
2MASS J01040695-6522272	12.447	13.95	8.532	-4.489	0.001	0.006	0.624	Bou22
2MASS J02004725-1021209	12.778	14.113	9.092	-4.791	0.001	0.188	14.793	Bou22
2MASS J02014384-1017295	13.026	14.477	9.189	-4.54	0.001	0.034	3.152	Bou22
2MASS J02125458+0000167	12.096	13.58	8.168	-4.635	0.001	0.048	4.732	Bou22
2MASS J02411510-0432177	12.251	13.79	8.246	-4.427	0.001	0.004	0.4	Bou22
2MASS J03100305-2341308	12.23	13.5	8.567	-4.234	0.001	0.028	2.083	Bou22
2MASS J03205178-6351524	12.087	13.433	8.195	-5.629	0.004	1.029	91.622	Bou22
2MASS J05015746-0656459	10.649	12.196	6.736	-5.005	0.002	0.875	88.5	Bou22

Table 1. First 10 rows of the dataset used in this work. This data is avalible as a machine readable supliment to this article.

Figure 5. Rotational Periods against G magnitude for all stars with rotational periods (top). Standard deviation of rotational period within magnitude bin (bottom).**The location of the Gap as identified in literature is shown by the hatched region ($\sim$ 10-10.5 M_G).**

Figure 6. Rossby number vs. G magnitude for all stars with rotational periods and V-K colors on Simbad. Dashed lines represent the hypothesized region of decreased rotation.**The location of the Gap as identified in literature is shown by the hatched region ($\sim$ 10-10.5 M_G).**

tions (R $\sim$ 16000) and a comparatively blue wavelength range [3].

Additionally, the sample we do have does not extend to as low mass as would be ideal. This presents a degeneracy between two potential causes for the observed increased star-to-star variability. One option, as presented above and elaborated on in the following section, is that this is due to kissing instabilities. However, another possibility is that this increased variability is intrinsic to the magnetic fields of fully convective stars. This al-

tical power of our analysis. This is primarily due to the relative difficulty of obtaining Ca II H&K measurements compared to obtaining $H\alpha$ measurements. Reliable measurements require both high spectral resolu-

_____

[3] wrt. to what many spectrographs cover. There is no unified resource listing currently commissioned spectrographs; however, it is somewhat hard to source glass which transmits well at H&K wavelengths limiting the lower wavelength of most spectrographs.

ternate option may be further supported by the shape of the magnetic activity spread vs. G magnitude relation. Convective kissing instabilities are not expected to continue to much lower masses than the fully convective transition mass. The fact that the increase in variance which we observe continues to much fainter magnitudes would therefore be somewhat surprising in a purely convective kissing instability driven framework (though the degeneracy between potentially physically driven increase in variance and increase in variance due to the noise-magnitude relation complicates attempts to constrain this.) There is limited discussion in the literature of overall magnetic field strength spanning the fully convective transition mass; however, Shulyak et al. (2019) present estimated magnetic field strengths for 47 M dwarfs, spanning a larger area around the convective transition region and their dataset does not indicate a inherently increased variability for fully convective stars.

3. MODELING

One of the most pressing questions related to this work is whether or not the increased star-to-star variability in the activity metric and the Jao Gap, which are coincident in magnitude, are driven by the same underlying mechanism. The challenge when addressing this question arises from current computational limitations. Specifically, the kinds of three dimensional magneto-hydrodynamical simulations — which would be needed to derive the effects of convective kissing instabilities on the magnetic field of the star — are infeasible to run over gigayear timescales while maintaining thermal timescale resolutions needed to resolve periodic mixing events.

In order to address this and answer the specific question of *could kissing instabilities result in increased star-to-star variability of the magnetic field*, we adopt a very simple toy model. Kissing instabilities result in a transient radiative zone separating the core of a star (convective) from its envelope (convective). When this radiative zone breaks down two important things happen: one, the entire star becomes mechanically coupled, and two, convective currents can now move over the entire radius of the star. Jao et al. (2023) propose that this mechanical coupling may allow the star's core to act as an angular momentum sink thus accelerating a stars spin down and resulting in anomalously low Hα emission.

Regardless of the exact mechanism by which the magnetic field may be affected, it is reasonable to expect that both the mechanical coupling and the change to the scale of convective currents will have some effect on the star's magnetic field. On a microscopic scale both of these will change how packets of charge within a star move and may serve to disrupt a stable dynamo.
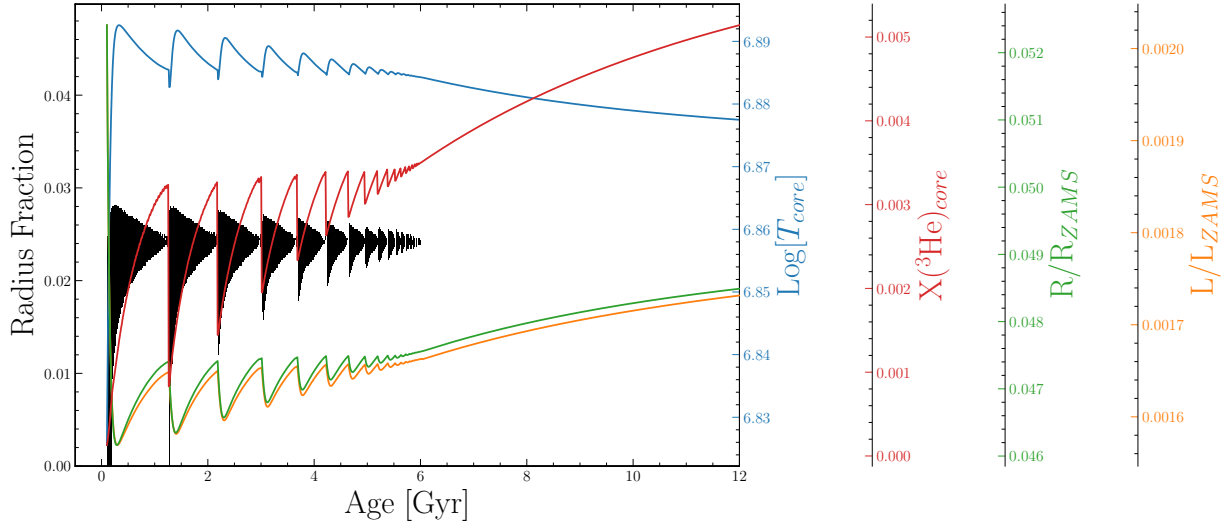
Therefore, in the model we present here we make only one primary assumption: *every mixing event may modify the star's magnetic field by some amount*. Within our model this assumption manifests as a random linear perturbation applied to some base magnetic field at every mixing event. The strength of this perturbation is sampled from a normal distribution with some standard deviation, σ_B.

Synthetic stars are sampled from a grid of stellar models evolved using the Dartmouth Stellar Evolution Program (DSEP) with similar parameters to those used in Boudreaux & Chaboyer (2023). Each stellar model was evolved using a high temporal resolution (timesteps no larger than 10,000 years) and typical numerical tolerances of one part in 10^5. Each model was based on a GS98 (Grevesse & Sauval 1998) solar composition with a mass range from 0.3 $M_\odot$ to 0.4 $M_\odot$. Finally, models adopt OPLIB high temperature radiative opacities, Ferguson 2004 low temperature radiative opacities, and include both atomic diffusion and gravitational settling. A Kippenhan-Iben diagram showing the structural evolution of a model within the Gap is shown in Figure 7.
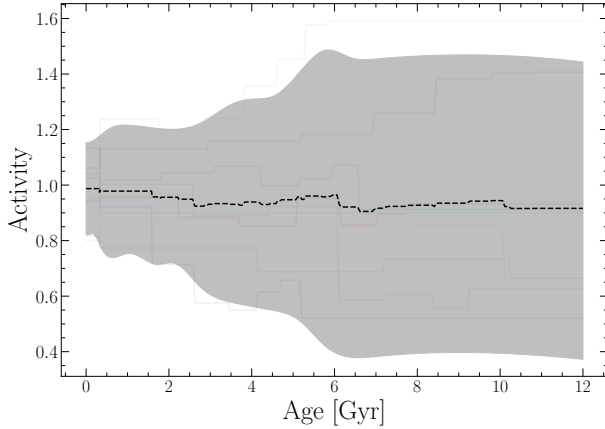
Each synthetic star is assigned some base magnetic activity ($B_0 \sim \mathcal{N}(1, \sigma_B)$) and then the number of mixing events before some age t are counted based on local maxima in the core temperature. The toy magnetic activity at age t for the model is given in Equation 2. An example of the magnetic evolution resulting from this model is given in Figure 8. Fundamentally, this model presents magnetic activity variation due to mixing events as a random walk and therefore results will increasing divergence over time.

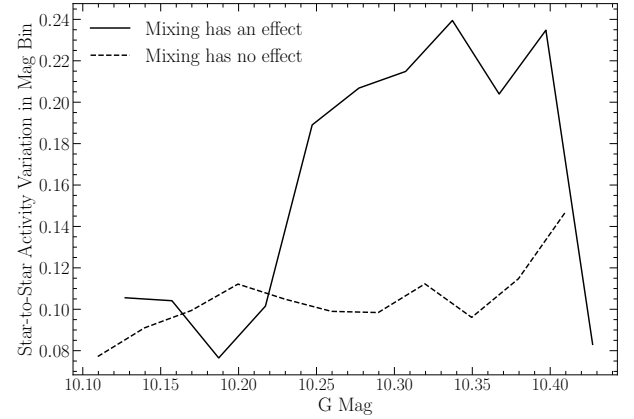$$B(t) = B_0 + \sum_i B_i \sim \mathcal{N}(1, \sigma_B) \qquad (2)$$

Applying the same analysis to these models as was done to the observations as described in Section 2 we find that this simple model results in a qualitatively similar trend in the standard deviation vs. Magnitude graph (Figure 9). In order to reproduce the approximately 50 percent change to the spread of the activity metric observed in the combined dataset in section 2 a distribution with a standard deviation of 0.1 is required when sampling the change in the magnetic activity metric at each mixing event. This corresponds to 68 percent of mixing events modifying the activity strength by 10 percent or less. The interpretation here is important: what this qualitative similarity demonstrates is that it may be reasonable to expect kissing instabilities to result in the observed increased star-to-star variation. Importantly, we are not able to claim that kissing instabilities *do* lead

Figure 7. Kippenhan-Iben diagram for a 0.345 solar mass star. Note the periodic mixing events (where the plotted curves peak).

Figure 8. Example of the toy model presented here resulting in increased divergence between stars magnetic fields. The shaded region represents the maximum spread in the two point correlation function at each age.

Figure 9. Toy model results showing a qualitatively similar discontinuity in the star-to-star magnetic activity variability.

to these increased variations, only that they reasonably could. Further modeling, observational, and theoretical efforts will be needed to more definitively answer this question.

3.1. *Limitations*

The model presented in this paper is very limited and it is important to keep these limitations in mind when interpreting the results presented here. Some of the main challenges which should be leveled at this model are the assumption that the magnetic field will be altered by some small random perturbation at every mixing event. This assumption was informed by the large number of free parameters available to a physical star during the establishment of a large scale magnetic field and the as-

sociated likely stochastic nature of that process. However, it is similarly believable that the magnetic field will tend to alter in a uniform manner at each mixing event. For example, since differential rotation is generally proportional to the temperature gradient within a star and activity is strongly coupled to differential rotation then it may be that as the radiative zone reforms over thermal timescales the homogenization of angular momentum throughout the star results in overall lower amounts of differential rotation each after mixing event than would otherwise be present.

Moreover, this model does not consider how other degenerate sources of magnetic evolution such as stellar spin down, relaxation, or coronal heating may effect star-to-star variability. These could conceivably lead to a similar increase in star-to-star variability which is coincident with the Jao Gap magnitude as the switch from

fully to partially convective may effect efficiency of these process.

Additionally, there are challenges with this toy model that originate from the stellar evolutionary model. Observations of the Jao Gap show that the feature is not perpendicular to the magnitude axis; rather, it is inversely proportional to the color. No models of the Jao Gap published at the time of writing capture this color dependency and *what causes this color dependency* remains one of the most pressing questions relating to the underlying physics. This non captured physics is one potential explanation for why the magnitude where our model predicts the increase in variability is not in agreement with where the variability jump exists in the data.

Finally, we have not considered detailed descriptions of the dynamos of stars. The magnetohydrodynamical modeling which would be required to model the evolution of the magnetic field of these stars at thermal timescale resolutions over gigayears is currently beyond the ability of practical computing. Therefore future work should focus on limited modeling which may inform the evolution of the magnetic field directly around the time of a mixing event.

4. CONCLUSION

It is, at this point, well established that the Jao Gap may provide a unique view of the interiors of stars for which other probes, such as seismology, fail. However, it has only recently become clear that the Gap may lend insight into not just structural changes within a star but also into the magnetic environment of the star. Jao et al. (2023) presented evidence that the physics driving the Gap might additionally result in a paucity of $H\alpha$ emission. These authors propose potential physical mechanisms which could explain this paucity, including the core of the star acting as an angular momentum sink during mixing events.

Here we have expanded upon this work by probing the degree and variability of Calcium II H&K emission around the Jao Gap. We lack the same statistical power of Jao et al.'s sample; however, by focusing on the star-to-star variability within magnitude bins we are able to retain statistical power. We find that there is an anomalous increase in variability at a G magnitude of ~ 11. This is only slightly below the observed mean gap magnitude.

Additionally, we propose a simple model to explain this variability. Making the assumption that the periodic convective mixing events will have some small but random effect on the overall magnetic field strength we are able to qualitatively reproduce the increase activity spread in a synthetic population of stars.

Software: The Dartmouth Stellar Evolution Program (`DSEP`) (Dotter et al. 2008), `BeautifulSoup` (Richardson 2007), `mechanize` (Chandra & Varanasi 2015), `FreeEOS` (Irwin 2012), `pyTOPSScrape` (Boudreaux 2022), `lightkurve` (Lightkurve Collaboration et al. 2018), `stella` (Feinstein et al. 2020a), `starspot` (Angus 2021; Angus & Garcia Soto 2023)

REFERENCES

Angus, R. 2021, Zenodo, doi: 10.5281/zenodo.4613887

Angus, R., & Garcia Soto, A. 2023, agarciasoto18/starrotate: Alternate Starrotate for Paper, v1.1, Zenodo, doi: 10.5281/zenodo.7697238. https://doi.org/10.5281/zenodo.7697238

Angus, R., Morton, T., Aigrain, S., Foreman-Mackey, D., & Rajpaul, V. 2018, Monthly Notices of the Royal Astronomical Society, 474, 2094, doi: 10.1093/mnras/stx2109

Astudillo-Defru, N., Delfosse, X., Bonfils, X., et al. 2017, A&A, 600, A13, doi: 10.1051/0004-6361/201527078

Baraffe, I., & Chabrier, G. 2018, A&A, 619, A177, doi: 10.1051/0004-6361/201834062

Barentsen, G., Hedges, C., Vinícius, Z., et al. 2020, KeplerGO/Lightkurve: Lightkurve v1.11.0, Zenodo, doi: 10.5281/zenodo.3836658

Boisse, I., Bouchy, F., Hébrard, G., et al. 2011, A&A, 528, A4, doi: 10.1051/0004-6361/201014354

Boudreaux, E. M., & Chaboyer, B. C. 2023, ApJ, 944, 129, doi: 10.3847/1538-4357/acb685

Boudreaux, E. M., Newton, E. R., Mondrik, N., Charbonneau, D., & Irwin, J. 2022, ApJ, 929, 80, doi: 10.3847/1538-4357/ac5cbf

Boudreaux, T. 2022, tboudreaux/pytopsscrape: pyTOPSScrape v1.0, v1.0, Zenodo, doi: 10.5281/zenodo.7094198. https://doi.org/10.5281/zenodo.7094198

Chabrier, G., & Küker, M. 2006, A&A, 446, 1027, doi: 10.1051/0004-6361:20042475

Chandra, R. V., & Varanasi, B. S. 2015, Python requests essentials (Packt Publishing Ltd)

Cretignier, M., Pietrow, A. G. M., & Aigrain, S. 2024, MNRAS, 527, 2940, doi: 10.1093/mnras/stad3292

Curtis, J. L., Agüeros, M. A., Matt, S. P., et al. 2020, ApJ, 904, 140, doi: 10.3847/1538-4357/abbf58

Dotter, A., Chaboyer, B., Jevremović, D., et al. 2008, The Astrophysical Journal Supplement Series, 178, 89

Dungee, R., van Saders, J., Gaidos, E., et al. 2022, ApJ, 938, 118, doi: 10.3847/1538-4357/ac90be

Feiden, G. A., Skidmore, K., & Jao, W.-C. 2021, ApJ, 907, 53, doi: 10.3847/1538-4357/abcc03

Feinstein, A., Montet, B., & Ansdell, M. 2020a, J. Open Source Softw., 5, 2347, doi: 10.21105/joss.02347

Feinstein, A. D., Montet, B. T., Ansdell, M., et al. 2020b, Astron. J., 160, 219, doi: 10.3847/1538-3881/abac0a

Fuhrmeister, B., Czesla, S., Schmitt, J. H. M. M., et al. 2019, A&A, 623, A24, doi: 10.1051/0004-6361/201834483

Gallet, F., Charbonnel, C., Amard, L., et al. 2017, A&A, 597, A14, doi: 10.1051/0004-6361/201629034

García Soto, A., Newton, E. R., Douglas, S. T., Burrows, A., & Kesseli, A. Y. 2023, AJ, 165, 192, doi: 10.3847/1538-3881/acc2ba

Grevesse, N., & Sauval, A. J. 1998, SSRv, 85, 161, doi: 10.1023/A:1005161325181

Houdebine, E. R., Mullan, D. J., Bercu, B., Paletou, F., & Gebran, M. 2017, ApJ, 837, 96, doi: 10.3847/1538-4357/aa5cad

Irwin, A. W. 2012, FreeEOS: Equation of State for stellar interiors calculations, Astrophysics Source Code Library, record ascl:1211.002. http://ascl.net/1211.002

Jao, W.-C., & Feiden, G. A. 2020, AJ, 160, 102, doi: 10.3847/1538-3881/aba192

—. 2021, Research Notes of the American Astronomical Society, 5, 124, doi: 10.3847/2515-5172/ac053a

Jao, W.-C., Henry, T. J., Gies, D. R., & Hambly, N. C. 2018, ApJL, 861, L11, doi: 10.3847/2041-8213/aacdf6

Jao, W.-C., Henry, T. J., White, R. J., et al. 2023, AJ, 166, 63, doi: 10.3847/1538-3881/ace2bb

Kislyakova, K. G., Noack, L., Johnstone, C. P., et al. 2017, Nature Astronomy, 1, 878, doi: 10.1038/s41550-017-0284-0

Kleeorin, N., Rogachevskii, I., Safiullin, N., Gershberg, R., & Porshnev, S. 2023, MNRAS, 526, 1601, doi: 10.1093/mnras/stad2708

Kochukhov, O. 2021, A&A Rv, 29, 1, doi: 10.1007/s00159-020-00130-3

Kumar, M., & Fares, R. 2023, MNRAS, 518, 3147, doi: 10.1093/mnras/stac2766

Kumar, V., Rajpurohit, A. S., Srivastava, M. K., Fernández-Trincado, J. G., & Queiroz, A. B. A. 2023, MNRAS, 524, 6085, doi: 10.1093/mnras/stad2222

Lammer, H., Güdel, M., Kulikov, Y., et al. 2012, Earth, Planets and Space, 64, 179, doi: 10.5047/eps.2011.04.002

Lightkurve Collaboration, Cardoso, J. V. d. M., Hedges, C., et al. 2018, Astrophysics Source Code Library, ascl:1812.013

Mansfield, S., & Kroupa, P. 2021, A&A, 650, A184, doi: 10.1051/0004-6361/202140536

Middelkoop, F. 1982, A&A, 107, 31

Newton, E. R., Irwin, J., Charbonneau, D., et al. 2016, ApJ, 821, 93, doi: 10.3847/0004-637X/821/2/93

Nutzman, P., & Charbonneau, D. 2008, PASP, 120, 317, doi: 10.1086/533420

Perdelwitz, V., Mittag, M., Tal-Or, L., et al. 2021, VizieR Online Data Catalog, J/A+A/652/A116, doi: 10.26093/cds/vizier.36520116

Rauscher, E., & Marcy, G. W. 2006, PASP, 118, 617, doi: 10.1086/503021

Richardson, L. 2007, April

Robertson, P., Stefansson, G., Mahadevan, S., et al. 2020, ApJ, 897, 125, doi: 10.3847/1538-4357/ab989f

Rodríguez-López, C. 2019, Frontiers in Astronomy and Space Sciences, 6, 76, doi: 10.3389/fspas.2019.00076

Rutten, R. G. M. 1984, A&A, 130, 353

Saar, S. H., & Linsky, J. L. 1985, ApJL, 299, L47, doi: 10.1086/184578

Salvatier, J., Wiecki, T. V., & Fonnesbeck, C. 2016, PeerJ Comput. Sci., 2, e55, doi: 10.7717/peerj-cs.55

Shulyak, D., Sokoloff, D., Kitchatinov, L., & Moss, D. 2015, MNRAS, 449, 3471, doi: 10.1093/mnras/stv585

Shulyak, D., Reiners, A., Nagel, E., et al. 2019, A&A, 626, A86, doi: 10.1051/0004-6361/201935315

Skrutskie, M. F., Cutri, R. M., Stiening, R., et al. 2006, AJ, 131, 1163, doi: 10.1086/498708

Spada, F., & Lanzafame, A. C. 2020, A&A, 636, A76, doi: 10.1051/0004-6361/201936384

Vaughan, A. H., Baliunas, S. L., Middelkoop, F., et al. 1981, ApJ, 250, 276, doi: 10.1086/159372

Winters, J. G., Henry, T. J., Jao, W.-C., et al. 2019, AJ, 157, 216, doi: 10.3847/1538-3881/ab05dc

702 Wright, N. J., Newton, E. R., Williams, P. K. G., Drake,
703 J. J., & Yadav, R. K. 2018, MNRAS, 479, 2351,
704 doi: 10.1093/mnras/sty1670